

CRYOGENIC TRANSFER LINE CHILLDOWN

N. T. Van Dresar^a and J. D. Siegwarth^b

^aNASA Glenn Research Center
Cleveland, OH 44253, USA

^bNational Institute of Standards and Technology
Boulder, CO 80305, USA

ABSTRACT

The transient behavior of a small-scale cryogenic transfer line was investigated during chilldown to cryogenic temperatures. The vacuum-jacketed apparatus consisted of a vertical tube followed by a near-horizontal tube. The tube diameter was 1 cm and the overall length was 4.4 m. The apparatus was equipped with view-ports in the near-horizontal section to allow visual observation of the flow patterns. Wall temperatures were measured at various locations along the length of the transfer line. Each test was conducted at a constant liquid volumetric flowrate at the transfer line inlet until saturation temperatures were obtained throughout the system. Liquid flowrate was varied by more than two orders of magnitude and resulted in chilldown times ranging from a few minutes to several hours. An optimum flowrate exists that minimizes liquid consumption during the chilldown process. At higher flowrates, there is insufficient time for heat transfer from the liquid to the wall and inefficiencies result from the greater amount of incompletely vaporized liquid passing through the system. At lower flowrates, chilldown time and total ambient heat leak into the system increase, which raises liquid consumption. The experimental values of liquid consumption are compared to analytical estimates. At low flowrates, the data compares favorably to a minimum consumption model while at high flowrates the maximum consumption model overpredicts hydrogen consumption and underpredicts nitrogen consumption.

INTRODUCTION

The chilldown of cryogenic transfer lines has long been of interest to cryogenic engineers as evidenced by numerous publications on various aspects of the subject [1-9]. A method to quickly estimate the minimum and maximum amounts of liquid required to chilldown a cryogenic pipeline is given by Jacobs [5] and Flynn [10]. These models equate the loss of internal energy of the transfer line wall to the cooling capacity of the cryogenic

liquid. More recently, experiments were conducted by the authors to obtain cryogenic two-phase heat transfer data [11-12]. In the course of these experiments, the transient behavior of the test apparatus (a long vacuum jacketed line) was investigated as the equipment was chilled down to cryogenic temperatures. Tests were conducted with both LN_2 and LH_2 over a wide range of fixed volumetric flowrates. The experimental results are reported herein.

APPARATUS

The apparatus was essentially a long slender tube that served as a flow path for the cryogenic test fluid. The upstream portion of the flow path was a vertical 1.3 cm diameter tube followed by a 0.95 cm diameter tube inclined 1.5° upward from horizontal. The vertical section was 1.3 m long while the near-horizontal section was 3.1 m long. A concentric copper radiation shield (4.4 cm diameter) surrounded the flow path. The tube and shield assembly was centered in a cylindrical stainless steel vacuum jacket (10.2 and 15.2 cm diameter). The upstream end of the flow path was connected to a bellows submerged in a supply dewar. The calibrated bellows was compressed at a steady rate by a stepper motor drive mechanism to produce a known volumetric flowrate at the flow path inlet. Flowrates for chilldown tests ranged from less than 0.1 to more than $10 \text{ cm}^3/\text{s}$. At the downstream end, the flow discharged into a liquid accumulator vented to the atmosphere through a backpressure regulator. A schematic of the apparatus is shown in Figure 1.

Several materials were used to construct the flow path. Much of the path was stainless steel tubing (used to minimize axial heat conduction) with copper tubing used in some locations. The heat transfer test section was made of brass tubing with short glass viewing sections on each end. In the upstream portion of the near-horizontal section, a preheater was installed to condition the fluid. The preheater shell was about 63 cm long and had an oval cross-section. The heater element also had an oval cross-section and was located within the bottom portion of the shell. The flow path from the dewar to the downstream end of the test section had a total mass of 1.17 kg. The composition was 48 percent stainless steel, 19 percent copper, 21 percent brass, 11 percent magnesium oxide (preheater heating element) and minor amounts of other materials. The internal volume of the

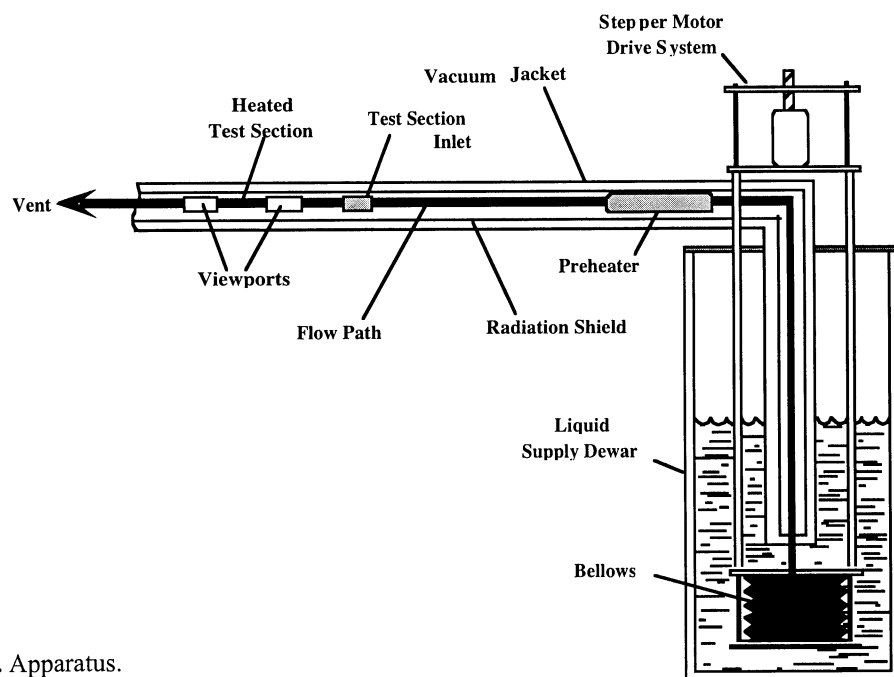


FIGURE 1. Apparatus.

apparatus from the bellows exit to the downstream end of the test section was 430 cm^3 . Further details concerning the apparatus construction are available elsewhere [11].

TEST CONDITIONS AND PROCEDURES

The apparatus was initially warm (250-290 K) with the flow path purged with either GN_2 or GH_2 as appropriate. Pressure inside the vacuum jacket was typically 10^{-4} to 10^{-3} Pa. The dewar and bellows were filled with either saturated LN_2 or LH_2 at atmospheric pressure. Discharge was to atmospheric pressure (80-85 kPa in Boulder, CO). Due to axial conduction through the flow path, the upstream end had an initial temperature gradient that extended from the bellows to the preheater region. Initial preheater inlet temperatures were 210-230 K. Chillydown was initiated by starting the stepper motor drive. Inlet volumetric flowrate was constant, but was varied over a range of more than two orders of magnitude from run to run. Sixteen tests were conducted with LN_2 over a flowrate range from 0.049 to $14.8\text{ cm}^3/\text{s}$. Six LH_2 tests were performed at flowrates from 0.124 to $14.8\text{ cm}^3/\text{s}$. There was no cooling flow through the radiation shield during chillydown and no electrical power was applied to the preheater or the test section to generate additional heat input. An analysis of steady state radiation heat transfer upon completion of chillydown indicated the vacuum jacket remained at ambient temperature while the radiation shield temperature dropped about 14 K. The maximum total heat leak into the chillydown system was approximately 6 W as calculated using a radiation model for long concentric cylinders [13].

Temperatures were recorded at five second intervals at the preheater inlet, test section inlet and the test section. Pressure was measured downstream of the test section and recorded. The two-phase flow was videotaped at the downstream window of the test section. Volumetric flowrate was calculated from the calibrated bellow displacement function and the selected stepper motor speed. Liquid consumption during chillydown was calculated using the known flowrate and elapsed time. An additional pressure sensor in the bellows was not considered to provide accurate absolute readings due to hydrostatic head effects, but was valuable for sensing the start of liquid outflow from the bellows. (Generally, a small quantity of trapped vapor in the top of the bellows would exit the bellows prior to liquid outflow.) The chillydown start time was taken to be at the onset of liquid outflow. Chillydown was considered complete when the downstream test section temperature attained a value equal to the liquid saturation temperature plus one percent of the difference between the initial and saturation temperatures.

TEST RESULTS

A representative example of the recorded wall temperatures during chillydown is shown in Figure 2. This example is for LH_2 flow at $0.74\text{ cm}^3/\text{s}$. As discussed above, the initial temperature at the preheater inlet was colder than at the remaining downstream positions. The preheater cooled to saturation temperature first, followed by the test section inlet and then the test section. At the highest flowrates, the temperature at the top of the test section slightly lagged the bottom temperature; otherwise, there were negligible circumferential temperature differences. It is informative to compare the test section temperature history to the observed flow patterns seen in the viewport adjacent to the downstream end of the test section. In the test shown in Figure 2, the initial flow pattern was single-phase vapor flow that transitioned to isolated liquid drops when 18.5 minutes had elapsed. The wall temperature was above the Leidenfrost point at this time and the

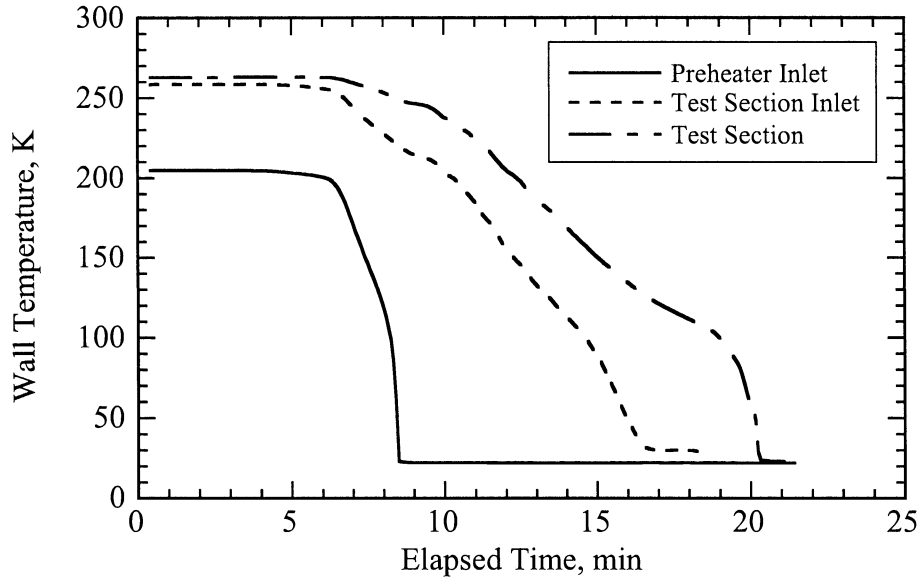


FIGURE 2. Example temperature transients (LH_2 flow at $0.74 \text{ cm}^3/\text{s}$).

liquid drops were supported by a vapor cushion. The flow then quickly underwent additional transitions to a wetted wall, slug flow and finally, plug flow. At all but the highest flowrates, single-phase liquid flow generally did not occur until back pressure was applied to the system and the radiation shield was cooled with a liquid bypass flow.

Figure 3 shows the chilldown time dependence on the inlet volumetric flowrate. As expected, the chilldown time decreases with increasing flowrate. The LN_2 data has an upward curvature that indicates a loss of cooling efficiency as the flowrate increases. This can be understood by realizing that as the flowrate increases the fluid has less contact time with the apparatus and a decreasing percentage of the fluid's sensible and latent heats are utilized. Complete chilldown of the apparatus was achieved with LN_2 over the entire range of test flowrates. The slope of the LH_2 curve is slightly steeper than the LN_2 curve. Furthermore, the LH_2 data has an interesting data point at a flowrate of $0.12 \text{ cm}^3/\text{s}$ where chilldown could not be attained throughout the apparatus due to the insufficient cooling capacity of the flow. In this case, the exiting flow was superheated vapor and the final steady temperature of the test section was 30 K above the saturation temperature.

Liquid consumption during chilldown is the product of chilldown time and volumetric flowrate. Figure 4 shows how the quantity of liquid required for chilldown depends on flowrate. LN_2 has a greater dependence on flowrate than LH_2 . Property differences between the test fluids are discussed later. The LH_2 curve shows the effect of insufficient flowrate at $0.12 \text{ cm}^3/\text{s}$. Complete chilldown was achieved at all test flowrates with LN_2 . However, with further reduction in the LN_2 flowrate, a point would be reached where the flowrate would not be sufficient to obtain complete chilldown. Knowing that complete chilldown with LH_2 was not achieved at $0.12 \text{ cm}^3/\text{s}$, but did occur at the next higher flowrate of $0.25 \text{ cm}^3/\text{s}$, it follows that the heat leak can be estimated to be about 6 W using the liquid density and heat of vaporization. This is in good agreement with the analytical estimate given earlier. Flynn [14] observes that there is little difference in heat leak for LN_2 and LH_2 vacuum jacketed transfer lines. Assuming this applies to the present apparatus, the minimum flowrate to achieve complete chilldown for LN_2 would be about $0.04 \text{ cm}^3/\text{s}$, which is slightly less than the minimum test flowrate.

The LN_2 curve on Figure 4 has a minimum near $0.2 \text{ cm}^3/\text{s}$ while the minimum for LH_2 appears somewhat higher based on the more limited data. At flowrates less than these, liquid quantity increases with decreasing flowrate. This is due to the increasing

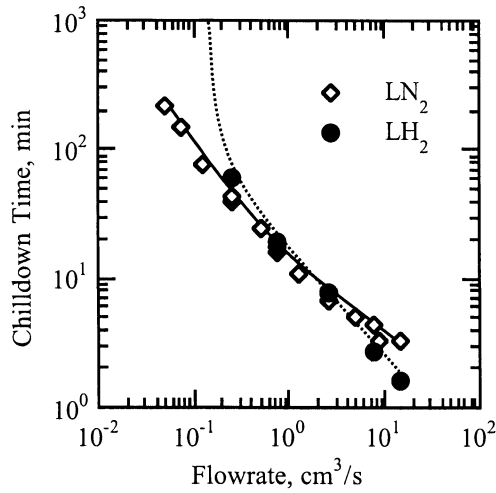


FIGURE 3. Chillum Time Dependence on Flowrate.

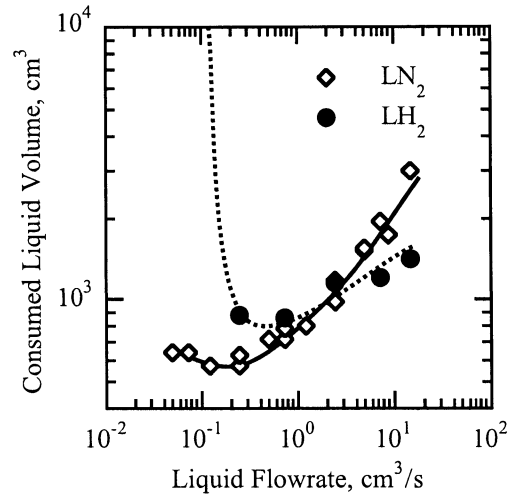


FIGURE 4. Liquid Consumption Dependence on Flowrate.

significance of environmental heat leak into the apparatus as a result of increasing chilldown time. From the limited amount of data of the present work, it is suggested that the optimum flowrate is about 3-5 times the minimum flowrate required to balance the total heat leak.

FLOW OBSERVATIONS

The observed characteristics of the flow transitions during chilldown varied significantly with flowrate for both test fluids. In all cases, the flow seen through the viewport downstream of the test section was initially all vapor since the liquid inlet flow was vaporized in the warm upstream portion of the apparatus. With LH_2 , the lowest flowrate ($0.12 \text{ cm}^3/\text{s}$) was insufficient to attain chilldown and the observed flow at the viewport was always vapor. At the next higher flowrate of $0.25 \text{ cm}^3/\text{s}$, a liquid front appeared 60 min. after startup. This liquid front was first seen as a shallow liquid layer that wetted the bottom of the tube as the leading edge passed through the glass section. The liquid surface was horizontal and the depth of liquid gradually increased as liquid was pumped into the flow path by the bellows. There was no evidence of nucleate or film boiling near the front. Temperature measurements indicate that the tube wall was cooled to the saturation temperature by the cold vapor flowing ahead of the front and that local chilldown was complete prior to the arrival of the liquid front. Phase change was apparently limited to evaporation at the liquid surface. At a flowrate of $0.74 \text{ cm}^3/\text{s}$, the first appearance of liquid occurred as liquid droplets rolling through the glass tube 18 min. after startup. In this case, the wall temperature was less than the initial value but above the Leidenfrost point. The liquid droplets were supported by a vapor film and film boiling was the primary heat transfer mechanism. After the wall temperature dropped below the Leidenfrost point, the liquid flow became a continuous stratified wavy flow. The liquid surface became smoother as the liquid height increased. When the chilldown was nearly complete, infrequent bursts of annular or slug flow occurred followed by transition to plug flow after chilldown was completed. At these lower flowrates (0.25 and $0.74 \text{ cm}^3/\text{s}$), the upper portion of the tube appears to experience a significant amount of cooling by gaseous convection or wall conduction to the lower portion of the tube.

At the higher flowrates of 2.5, 7.4 and 15 cm³/s, the first appearance of liquid occurred as a high-speed burst of a liquid droplet cloud (mist). After the initial burst, the density and frequency of the droplet cloud bursts increased. The initial droplet cloud sightings occurred at 6, 2 and 1 min., respectively, after startup. As the chilldown continued, a thin liquid layer developed on the tube bottom. This wetting of the tube bottom was sometimes intermittent for a brief interval, but soon followed by a period of steady liquid presence at the tube bottom. When chilldown was nearly completed, bursts of annular or slug-like flow completely wetted the tube wall. These events were later followed by a transition to plug flow after chilldown was complete. At high flowrates, the observed void fraction decreased to zero or near-zero, while at the low flowrates it was substantially higher since the heat leak approaches the magnitude of the flow's cooling capacity (mass flowrate times heat of vaporization).

The flow observations with LN₂ were similar to LH₂, but with a few differences. With LN₂ at the lowest flowrates (0.049 and 0.074 cm³/s) the liquid front advanced unevenly and the initial liquid layer(s) would dry up completely. At flowrates from 0.12 to 0.74 cm³/s, larger quantities of liquid were observed prior to the transition from film to nucleate boiling. The first appearance of liquid was as elongated droplets above the Leidenfrost point. Brief occurrences of bubble formation on the wall could be observed immediately after the boiling transition. At the highest flowrates (2.5 to 14.8 cm³/s), the first appearance of liquid took place at much higher speed. Gas velocities for N₂ are higher due to the liquid-to-vapor density ratio of N₂ being more than three times that of H₂. The liquid was either suspended as mist in the high-speed gas core flow or it was streaming along the wall as a film. The droplet clouds or wall films contained increasing amounts of liquid as the process continued. There was then a rather abrupt transition to slug flow followed by plug flow and completion of chilldown. At the highest flowrate, transition to single-phase liquid flow occurred prior to chilldown completion and a substantial amount of liquid was discharged.

COMPARISON TO LIQUID CONSUMPTION ESTIMATES

Since the experimental results indicate that heat leak becomes an important factor at low flowrates, Flynn's minimum and maximum consumption models [10] were modified by including an additional term for the extra quantity of liquid required to offset the environmental heat input. This term was equal to the product of the chilldown time, average total heat leak rate and the inverse of the heat of vaporization per unit volume. The average heat leak rate was estimated to be two-thirds of the maximum heat leak rate (4 W). The heat leak was initially zero and increased to the maximum at the end of chilldown; however the average value is not one-half of the maximum since the wall specific heat is temperature dependent. The average heat leak was obtained by numerically integrating the specific heat curve of the dominant wall material (stainless steel) to find the midpoint temperature (at which the decrease in wall heat capacity is one-half the maximum decrease occurring at complete chilldown). This midpoint temperature was then used in the concentric cylinder radiation model mentioned earlier to obtain the average heat leak. The minimum model assumes both the heat of vaporization and all of the sensible heat of the vaporized liquid are available for cooling. It also includes the liquid volume required to offset the heat leak. The minimum model assumes the transfer line contains only vapor at the completion of chilldown.

Flynn's maximum model assumes only the heat of vaporization is available to cool the transfer line. This was modified to include the additional heat leak term described above. A

second term was added that is equal to the internal volume of the transfer line. This term was added to the maximum model because the apparatus could contain at least some liquid at the time chilldown was achieved. The maximum model thus accounts for the liquid's heat of vaporization, but none of the sensible heat of the generated vapor, and assumes the transfer line is filled with liquid at the completion of chilldown. The maximum model includes the same correction for heat leak as the minimum model.

Both models were numerically evaluated using the temperature dependent specific heats of the four primary materials used in the apparatus construction and the known amounts of each material. The liquid consumption models are compared to the LN_2 and LH_2 experimental results in Figures 5 and 6 respectively. The upward trend of the minimum curves shows the significance of heat leak at low flowrates. The proximity of the experimental data to the minimum curve for both fluids indicates an efficient chilldown process at the lower end of the flowrate range. Figure 5 indicates that the chilldown process was very inefficient at high flowrates for LN_2 , while Figure 6 indicates that the same volumetric flowrates for LH_2 result in liquid consumption well below the estimated maximum. It was observed that a significant amount of LN_2 exited the apparatus prior to chilldown completion and this is the primary cause of the results exceeding the maximum curve for LN_2 . The greater liquid-to-vapor density ratio for N_2 discussed above causes higher vapor velocities for N_2 and more liquid is carried through the transfer line without vaporization than takes place for H_2 at the same volumetric flowrate. However, liquid discharge was also observed at high flowrates with H_2 . Compared to N_2 , H_2 has a lower heat of vaporization per unit liquid volume, but a higher heat capacity for the vapor and less entrainment of the liquid since vapor velocities are lower. The explanation for the overprediction of the maximum model under the conditions of LH_2 discharge is that the sensible heat capacity of vaporized H_2 is neglected in the model, even though it is a significant factor at all flowrates.

CONCLUSIONS

Experimental data has been obtained for the time and required amount of liquid hydrogen or nitrogen necessary to completely chill down a long vacuum jacketed cryogenic transfer line. At high volumetric flowrate at the liquid inlet, excessive amounts of liquid will pass through the line without vaporization. If the flowrate is too low, the required time

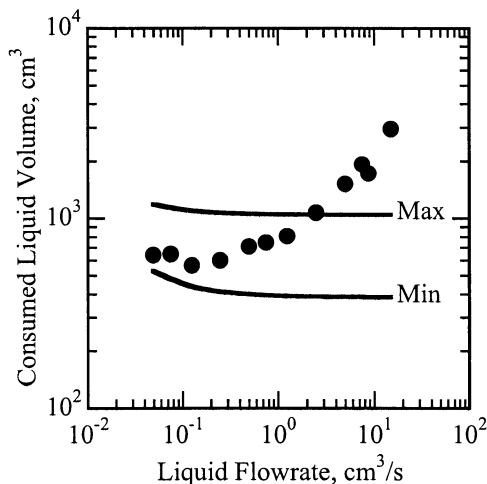


FIGURE 5. Comparison of Minimum and Maximum Estimates to LN_2 Experimental Data.

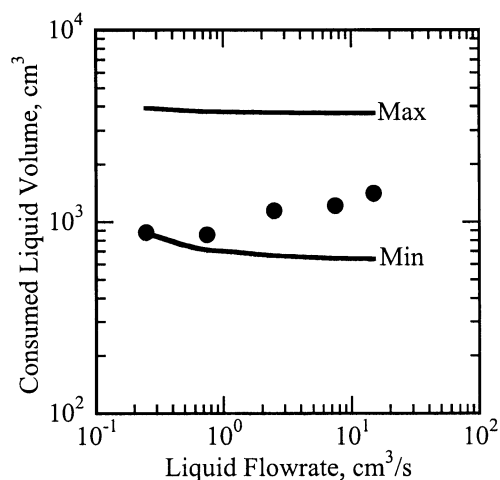


FIGURE 6. Comparison of Minimum and Maximum Estimates to LH_2 Experimental Data.

becomes substantial and liquid vaporization due to heat leak becomes a significant factor. Also, if the flowrate is less than the rate required to balance the heat leak, complete chilldown can not be achieved. The present results indicate that an optimum flowrate exists at which the amount of consumed liquid for chilldown is minimized. The limited amount of data suggests that the optimum volumetric flowrate is about 3-5 times the flowrate necessary to balance the total heat leak in a completely chilled down transfer line.

Simple models to estimate the amount of liquid required for chilldown are compared to the experimental results. At low flowrates, a minimum consumption model based on Flynn's model with an additional term to account for the liquid vaporized by heat leak provides a reasonably good lower bound for both nitrogen and hydrogen. A maximum model based on Flynn's model with the added heat leak term as well as a term to account for the liquid volume contained within the transfer line underpredicts the nitrogen results at high flowrate primarily due to the large amounts of entrained liquid carried through the system resulting from the high vapor discharge velocities. The maximum model significantly overpredicts the hydrogen results at high flowrate in spite of observed liquid discharge from the transfer line. The overprediction is largely due to the omission of the sensible heat of the vaporized liquid that for hydrogen is much greater than its heat of vaporization.

REFERENCES

1. Jacobs, R.B., Richards, R.J., and Schwartz, S.B., "The Transfer of Liquified Gases," in *Advances in Cryogenic Engineering*, edited by K.D. Timmerhaus, Plenum Press, New York, **1**, 87-94, (1956).
2. Burke, J.C., Byrnes, W.R., Post, A.H., and Ruccia, F.E., "Pressurized Cooldown of Cryogenic Transfer Line," in *Advances in Cryogenic Engineering*, edited by K.D. Timmerhaus, Plenum Press, New York, **4**, 378-394, (1959).
3. Drake, E.M., Ruccia, F.E., and Ruder, J.M., "Presurized Cool-Down of a Cryogenic Liquid Transfer System Containing Vertical Sections," in *Advances in Cryogenic Engineering*, edited by K.D. Timmerhaus, Plenum Press, New York, **6**, 323-333, (1961).
4. Bronson, J.C., Edeskuty, F.J., Fretwell, E.F., Hammel, E.F., Keller, W.E., Meier, K.L., Schuch, A.F., and Willis, W.L., "Problems in Cool-down of Cryogenic Systems," in *Advances in Cryogenic Engineering*, edited by K.D. Timmerhaus, Plenum Press, New York, **7**, 198-205, (1962).
5. Jacobs, R.B., "Liquid Requirements for the Cool-Down of Cryogenic Equipment," in *Advances in Cryogenic Engineering*, edited by K.D. Timmerhaus, Plenum Press, New York, **8**, 529-535, (1963).
6. Chi, J.W.H., "Cooldown Temperatures and Cooldown Time During Mist Flow," in *Advances in Cryogenic Engineering*, edited by K.D. Timmerhaus, Plenum Press, New York, **10**, 330-340, (1965).
7. Steward, W.G., Smith, R.V., and Brennan, J.A., "Cooldown Transients in Cryogenic Transfer Lines," in *Advances in Cryogenic Engineering*, edited by K.D. Timmerhaus, Plenum Press, New York, **15**, 354-362, (1970).
8. Srinivasan, K., Rao, S., and Krishna Murthy M.V., "Analytical and Experimental Investigation on Cool-Down of Short Cryogenic Transfer Lines," *Cryogenics*, **14**, pp. 489-494, (1974).
9. Krishnamurthy M.V., Chandra, R., Jacob, S., Kasthurirengan, S., and Karunanithi, R., "Experimental Studies on Cool-Down and Mass Flow Characteristics of a Demountable Liquid Nitrogen Transfer Line," *Cryogenics*, **36**, pp. 453-441, (1996).
10. Flynn, T.M., *Cryogenic Engineering*, Marcel Decker, New York, 1996, pp. 67-69.
11. Van Dresar, N.T. and Siegwarth, J.D. "Near-Horizontal, Two-Phase Flow Patterns of Nitrogen and Hydrogen at Low Mass and Heat Flux," NASA/TP—2001-210380, 2001.
12. Van Dresar, N.T., Siegwarth, J.D. and Hasan, M.M. "Convective Heat Transfer Coefficients for Near-Horizontal Two-Phase Flow of Nitrogen and Hydrogen at Low Mass and Heat Flux," *Cryogenics*, **41**, pp. 805-811 (2002).
13. Incropera, F.P. and DeWitt, D.P., *Fundamentals of Heat and Mass Transfer*, 4th edition, Wiley, New York, 1996, p. 739.
14. Flynn, T.M., *Cryogenic Engineering*, Marcel Decker, New York, 1996, p. 64.